

ARTICLE

Regional patterns of seismic b-values variations in the Himalayan region (71.6°E – 95.5°E and 37.5°N – 26.6°N)

Ram Krishna Tiwari*, Anil Subedi, Dilip Parajuli, Santosh Dharel, Anil Neupane, Hari Subedi, Bishow Raj Timsina, and Harihar Paudyal

Department of Physics, Birendra Multiple Campus, Tribhuvan University, Bharatpur, Chitwan, Nepal

Abstract

This study conducts a detailed seismic hazard assessment of the Himalayan region. It focuses on studying how b-values, based on the Gutenberg–Richter law, vary throughout location and time. These fluctuations assist measuring tectonic stress and provide insights into the region's seismic activity. This research focuses on five Himalayan sub-regions: Far Western, Western, Central-I, Central-II, and Eastern. It incorporates earthquake data spanning 1964 – 2023 obtained from the International Seismological Centre. The data were de-clustered using the Reasenber method and examined by Maximum Likelihood Estimation. The results demonstrated considerable spatial variability in b-values across the Himalayan sub-regions. The Far Western Himalayas displayed the greatest b-value (0.93 ± 0.02), indicating frequent smaller earthquakes and lesser tectonic stress. In contrast, the Eastern (0.68 ± 0.02) and Central-I (0.69 ± 0.03) regions had the lowest b-values, implying more stress accumulation and a greater risk of future strong earthquakes. Temporal fluctuations, as a decrease in b-values preceding to the 2015 Gorkha earthquake (Mw 7.8) and a subsequent increase in Central-II (1.19 ± 0.03), highlighted the retention and release cycles. The Eastern Himalayas, particularly the Dhubri-Chungthang fault zone seismic gap in Bhutan, are considered a key high-risk zone. This region, with b-values ranging from 0.65 to 0.75, has remained unruptured since the 1934 Bihar-Nepal earthquake (Mw 8.4). The findings showed the influence of the continual convergence of the Indian and Eurasian plates (~20 mm/year) on strain heterogeneity. This study underlines the vital demand for intensive seismic monitoring, resilient infrastructure, and disaster readiness in low b-value areas to alleviate catastrophic risks in one of the globe's most tectonically active regions.

*Corresponding author:

Ram Krishna Tiwari
(ram.tiwari@bimc.tu.edu.np)

Citation: Tiwari RK, Subedi A, Parajuli D, *et al.* Regional patterns of seismic b-values variations in the Himalayan region (71.6°E – 95.5°E and 37.5°N – 26.6°N). *J Seismic Explor.*
doi: 10.36922/JSE025210006

Received: May 25, 2025

Revised: July 5, 2025

Accepted: July 8, 2025

Published online: July 28, 2025

Copyright: © 2025 Author(s). This is an Open-Access article distributed under the terms of the Creative Commons Attribution License, permitting distribution, and reproduction in any medium, provided the original work is properly cited.

Publisher's Note: AccScience Publishing remains neutral with regard to jurisdictional claims in published maps and institutional affiliations.

Keywords: b-value; Gutenberg–Richter law; Himalayan region

1. Introduction

The Himalayan Mountain Range, the tallest mountain chain in the world, traverses five countries – India, Nepal, Bhutan, China (Tibet), and Pakistan – and extends over 2,400 km in southern Asia.¹ The continual collision between the Indian and Eurasian tectonic plates, which began around 50 million years ago (Mya) after the Neo-Tethys Ocean closed, is responsible for its construction.² The Indian Plate subducted northward beneath Eurasia between 70 and 50 Mya, closing the Tethys Ocean and leaving

behind the Indus-Tsangpo Suture Zone, a geological indicator of the ancient oceanic crust, was the primary step in the orogenesis of the Himalayas.³ The continental collision phase (50 – 40 Mya) resulted in massive crustal shortening, folding, and thrust faulting, which uplifted the Greater Himalayas through systems, such as the Main Central Thrust, while the Main Boundary Thrust and Main Frontal Thrust distinguish the Lesser Himalayas and the young, sediment-rich Siwalik Hills, respectively.^{4,5} Ongoing northward convergence of the Indian Plate at 5 – 10 mm/year sustains tectonic activity, driving uplift of peaks, such as Mount Everest and accumulating stress along major faults, such as the Main Himalayan Thrust (MHT), a primary source of strong earthquakes.^{6,7} This dynamic process ensures continued seismic hazard in the region, exemplified by historical earthquakes and the persistent risk of future events as strain energy is episodically released.^{8,9}

An earthquake is defined as the sudden release of accumulated stress along locked tectonic plate boundaries or intraplate zones, where abrupt crustal movement generates seismic waves.^{9,10} In the Himalayas, this process is driven by the ongoing India-Eurasia collision, which has generated significant seismicity linked to strain release along the MHT.^{2,6} One of the notable seismic activities in the Himalayas is the 1905 Kangra earthquake (Mw 7.8), where a segment of the western Himalayan front was ruptured, releasing stress accumulation in the Kangra reentrant.^{11,12} The Bihar-Nepal earthquake (Mw 8.1) in 1934 involved slip along a ~250 km portion of the MHT, illuminating shallow decollement dynamics.¹³⁻¹⁶ The 1950 Assam-Tibet earthquake (Mw 8.6) highlights the complexity of oblique convergence near the eastern Himalayan syntaxis, where thrust and strike-slip faulting combine to produce bimodal faulting.^{17,18} The 2005 Kashmir earthquake (Mw 7.6) highlighted strain partitioning in the western syntaxis, with thrust and strike-slip components.^{8,19,20} Most recently, the 2015 Gorkha earthquake (Mw 7.8) in central Nepal ruptured a 150 km × 60 km patch of the MHT, leaving deeper segments unbroken and underscoring heterogeneous coupling.^{8,21-23} These events, spanning the MHT's strike, reveal segmented rupture behavior and variable locking depths, with GPS-derived convergence rates (~18 – 20 mm/year), suggesting ongoing strain accumulation.⁶

By analyzing the b-value in the Gutenberg–Richter law, this study aims to identify zones of differential stress accumulation, potential asperities, and fault maturity across the Himalayan region (71.6°E – 95.5°E and 26.6°N – 37.5°N), subdivided into five distinct sub-regions. Based on the probabilistic seismic hazard assessment report of India,

tectonic features, and geology, the region has been broadly divided into four sections,²⁶⁻²⁸ with the western section further subdivided for improved analysis. As a result, we have categorized the Himalayan region into five zones: Far Western, Western, Central-I, Central-II, and Eastern (Figure 1). Each of these zones has been defined based on distinct geological and tectonic characteristics to ensure a comprehensive assessment.

1.1. Frequency magnitude distribution

The frequency-magnitude distribution (FMD) of earthquakes²⁹ is a fundamental statistical relationship in seismology. It describes how the frequency of earthquakes scales with their magnitude, using the following equation:

$$\log N = a - bM \quad (1)$$

In Equation 1, N is the cumulative number of events having magnitude $\geq M$; M is the magnitude of earthquakes; the constant a is the seismicity of the region; and b is the b-value of the earthquake frequency magnitude distribution.²⁹ The b-value, a key parameter in the Gutenberg–Richter law, quantifies the relative frequency of small to large earthquakes, where a lower b-value indicates a higher likelihood of large-magnitude events due to elevated tectonic stress, while a higher b-value reflects frequent small earthquakes and lower crustal strain.³⁰⁻³² To assess regional stress accumulation and evaluate the seismic hazard potential, seismologists have analyzed spatial and temporal fluctuations in b-values around the globe. As an example, researchers analyzed spatiotemporal variations in b-value within the subducting slab before the 2003 Tokachi-oki earthquake (M 8.0), Japan, to identify precursory seismic signatures.³³ Similarly, the b-value anomalies were noticed before the Assam Earthquake on April 28, 2021.³⁴ In addition, the low b-value anomaly identified in the west of Gorkha highlights the zone with potentially strong seismic activity in the future.³⁵

2. Data and methods

An extensive earthquake catalogue covering a long period is essential for studying the seismic activity of any region. In this study, we focused on the Himalayas, located between 71.6°E and 95.5°E, and utilized earthquake data for the period from 1964 to 2023, from the International Seismological Centre catalogue.³⁶⁻³⁸ The earthquake magnitudes in the catalogue are reported in mb (body-wave magnitude). The dataset comprises both dependent (foreshocks and aftershocks) and independent (mainshocks) events, but to ensure accurate analysis, only independent earthquakes are considered by applying de-clustering using the Reasenber algorithm.³⁹ The de-clustering process was carried out in ZMAP

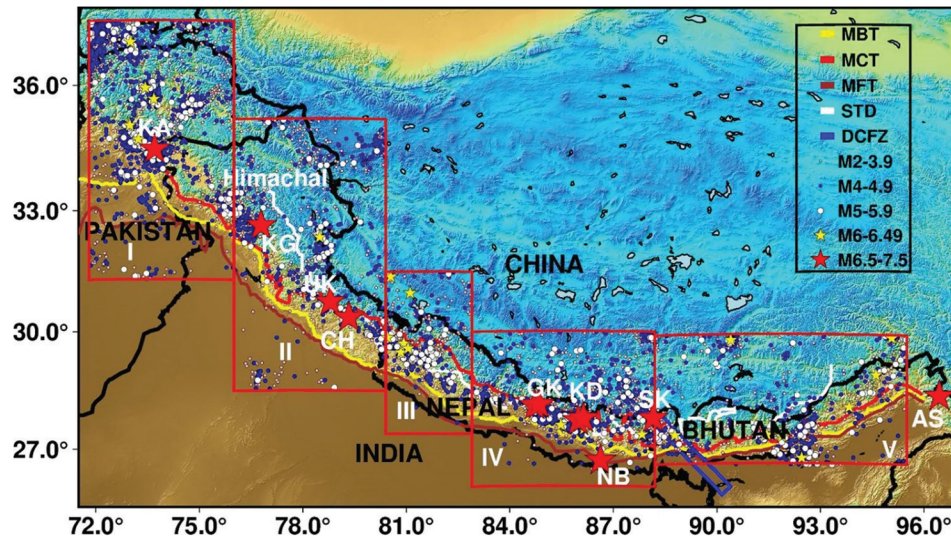


Figure 1. Study region with earthquake distribution. Red star indicates the earthquake >6.4 mb and notable past earthquakes, and red rectangular box are subdivided regions. UK stands for Mw 6.8 Uttar Kashi earthquake, CH stands for Mw 6.4 Chamoli earthquake, GK stands for Mw 7.8 Gorkha earthquake, NB stands for Mw 8.4 Nepal-Bihar earthquake, KA stands for Mw 7.6 Kashmir earthquake, SK stands for Mw 6.9 Sikkim earthquake, KG stands for Mw 7.8 Kangra earthquake, and AS stands for Mw 7.8 Assam earthquake. The blue rectangle stands for Dhubri-Chunghthang Fault Zone (DCFZ).^{24,25}

software (Swiss Seismological Service, Switzerland).⁴⁰ The segmented study regions are:

- (i) Far Western Himalayan region (31.3°N – 37.5°N and 71.6°E – 76°E): A total of 3445 earthquake events with a magnitude of 3.0 mb or greater were recorded. After applying the de-clustering process, 47 clusters were identified, and following the removal of dependent events, 2867 independent events were retained.
- (ii) Western Himalayan region (28.8°N – 35.2°N and 76°E – 80.2°E): A total of 1040 earthquake events with a magnitude of 3.0 mb or greater were recorded. After the de-clustering process, 24 clusters were identified, and following the removal of dependent events, 1004 independent events were retained.
- (iii) Central-I Himalayan region (27.4°N – 31.5°N and 80.2°E – 82.9°E): A total of 529 earthquake events with a magnitude of 3.0 mb or greater were recorded. After the de-clustering process, 11 clusters were identified, and following the removal of dependent events, 494 independent events were retained.
- (iv) Central-II Himalayan Region (26.03°N – 30°N and 82.9°E – 88.2°E): A total of 1482 earthquake events with a magnitude of 3.0 mb or greater were recorded. After the de-clustering process, 35 clusters were identified, and following the removal of dependent events, 1079 independent events were retained.
- (v) Eastern Himalayan region (26.6°N – 29.9°N and 88.2°E – 95.5°E): A total of 767 earthquake events with a magnitude of 3.0 mb or greater were recorded. After

the de-clustering process, 8 clusters were identified, and following the removal of dependent events, 706 independent events were retained.

The b-value was determined using the maximum likelihood estimate approach, which remains unaffected by large-magnitude earthquakes. In addition, the magnitude of completeness was computed using the first derivative of the frequency-magnitude curve.³² The formula^{41,42} for b-value estimation is as follows:

$$b = \frac{\log_{10} e}{M_a - (M - \frac{\Delta M}{2})} \quad (\text{II})$$

where M_a is the average of all magnitudes; M is the minimum magnitude in the catalogue; and ΔM is the binning width of the catalogue. The standard deviation in b-value (δb), as recommended elsewhere,⁴³ is provided in the following:

$$\delta b = 2.3b^2 \sqrt{\frac{\sum_i^N (M_i - M_a)^2}{n_s (n_s - 1)}} \quad (\text{III})$$

where M_i denotes the individual earthquake magnitudes; M_a is the average magnitude of all the earthquakes considered; and n_s refers to the total number of earthquake samples used in the calculation. The expression $\sum_i^N (M_i - M_a)^2$ represents the sum of the squared differences between each magnitude and the mean magnitude.

3. Results and discussion

As mentioned in the past literature, temporally declining b-values precede major earthquakes, signaling stress concentration,^{44,45} and spatially, low b-values correlate with locked, high-stress zones, while high b-values reflect fractured, aseismic regions.^{46,47} Together, these patterns highlight the utility of b-values in mapping stress heterogeneity and identifying seismogenic potential. To better understand these dynamics, we investigated spatial and temporal b-value variations in the Himalaya to

quantify stress heterogeneity and earthquake likelihood. The estimated b-values for all five regions (Far Western, Western, Central-I, Central-II, and Eastern) are illustrated in Figure 2, with their corresponding numerical values provided in Table 1.

The Far Western region (Figure 2A) exhibits the highest b-value (0.93 ± 0.02), indicating a predominance of small magnitude earthquakes, which is a common feature of tectonically active zones. Conversely, the Central-I (Figure 2C) and Eastern regions (Figure 2D)

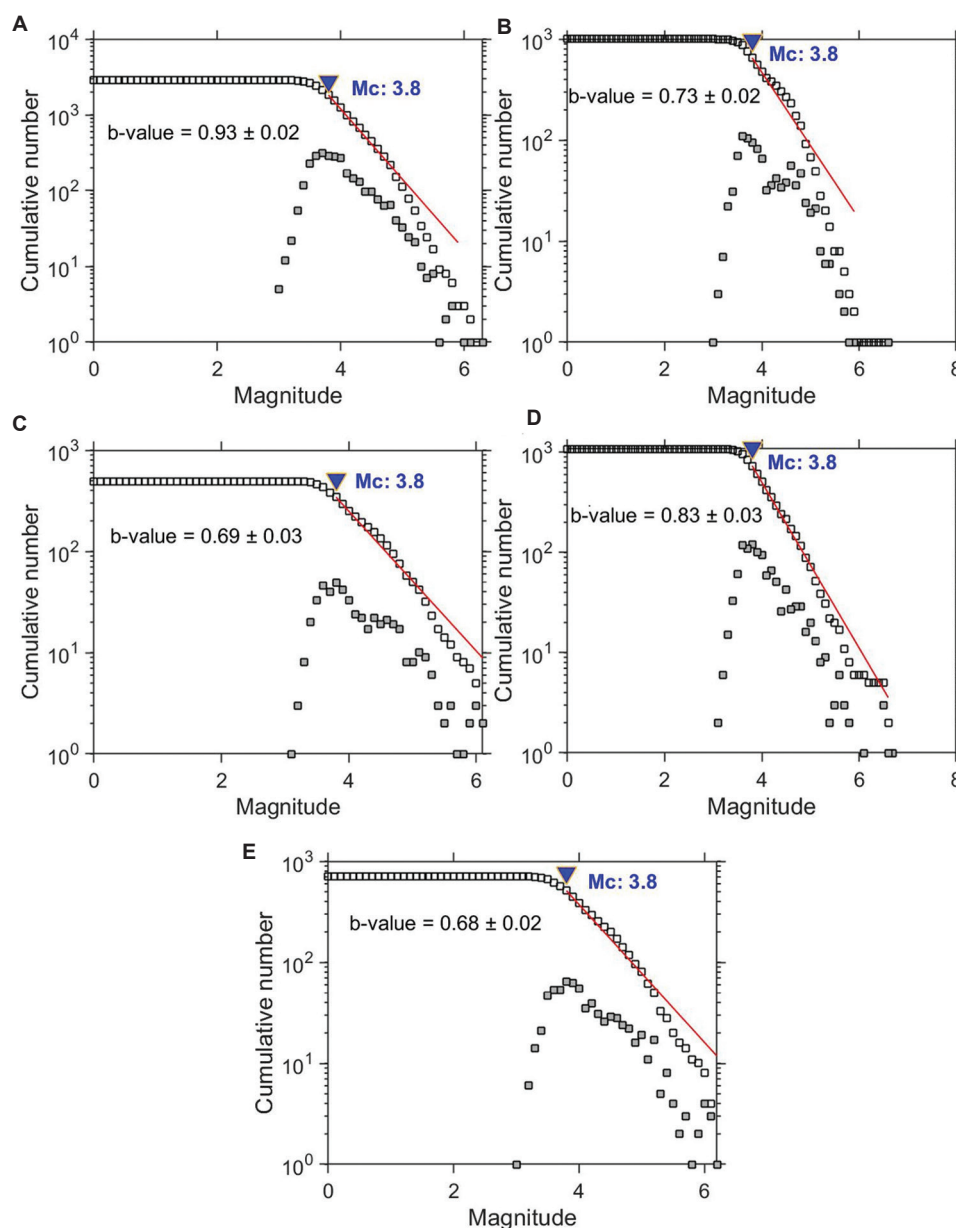


Figure 2. b-value and magnitude of completeness plots of Far Western Himalayan region (A), Western Himalayan Region (B), Central-I Himalayan Region (C), Central-II Himalayan Region (D), and Eastern Himalayan Region (E)

Table 1. b-value and magnitude of completeness in five regions of the Himalayan

Region	b-value	Magnitude of completeness (Mc)	Magnitude range (in M_b)
Far Western	0.93 ± 0.02	3.8	3 – 6.9
Western	0.73 ± 0.02	3.8	3 – 6.6
Central I	0.69 ± 0.03	3.8	3 – 6.1
Central II	0.83 ± 0.03	3.8	3 – 6.9
Eastern	0.68 ± 0.02	3.8	3 – 6.2

have the lowest b-values (0.69 ± 0.03 and 0.68 ± 0.02 , respectively), suggesting a lower frequency of small earthquakes and a greater potential for stress accumulation, which may contribute to the occurrence of larger seismic events.^{48,49} Meanwhile, the Western (Figure 2B) and Central-II (Figure 2D) regions demonstrate moderate b-values (0.73 ± 0.02 and 0.83 ± 0.03 , respectively), reflecting a more balanced seismic activity pattern.^{50,51} These variations in b-values provide crucial insights into seismic behavior and potential hazard levels across different regions. In the preceding work, b-values calculated for the Himalayan region from 1900 to 2015, were reported as 0.98, 0.86, 0.85, and 0.74 for the Western, Central-I, Central-II, and Eastern zones, respectively, by Pudi *et al.*²⁶ Similarly, other studies have analyzed b-values across the Himalayas, demonstrating differences in stress and seismic hazard. Tiwari and Paudyal⁵² discovered a b-value of 0.68 ± 0.03 in western Nepal (central Himalaya), indicating a high-stress zone with locked faults. Kumar and Sharma⁵³ reported b-values ranging from 0.7 to 1.1 in central Nepal (central Himalaya), showing stress heterogeneity after the 2015 Gorkha earthquake. Pathak *et al.*⁵⁴ discovered a high-stress environment in the Kumaun region of the western Himalayas, with a b-value of 0.59 ± 0.11 . Similarly, Yadav *et al.*⁵⁵ reported low b-values ranging from 0.6 to 0.7 in the northeastern Himalayas, particularly along the MHT, indicating locked faults and high seismic potential. These low b-values across locations show the Himalayan belt's enormous stress and earthquake vulnerability.

The temporal fluctuations in b-values over the study region indicate varying stress regimes and seismic activities (Figure 3).

In the Far Western Himalaya (Figure 3A), a decrease in b-value from 1.04 (July 15, 1990) to 0.97 (November 11, 2015) during the 1980 – 2020 period signifies ongoing stress accumulation along the MHT.⁵⁶ The initial elevated b-value indicated stress relaxation through frequent little earthquakes, but the subsequent decline suggested an increase in strain concentration. The Western Himalayas (Figure 3B) exhibited a low b-value of 0.84

on August 30, 1995, associated with stress accumulation preceding the 1991 Uttarkashi (Mw 6.8) and 1999 Chamoli (Mw 6.4) earthquakes, influenced by locked parts of the Main Central Thrust.^{57,58}

In the Central-I Himalayas (Figure 3C), the b-value of 0.94 recorded on December 14, 2006, throughout the period from 1995 to 2015 indicated moderate stress conditions with ongoing strain building along the MHT. In contrast, the Central-II Himalayas (Figure 3D) saw a significant increase in the b-value to 1.19 on May 10, 2015, following the Gorkha earthquake, indicating stress release through aftershocks.⁵⁹ The Eastern Himalayas (Figure 3E) exhibited consistently elevated and constant b-values (0.97 in 2014; 0.99 in 2016) from 1990 to 2015, indicating reduced stress attributable to crustal variability. This region constitutes a seismic gap that has remained unruptured since the 1934 Bihar-Nepal earthquake (Mw 8.4), with locked faults quietly collecting strain.^{8,14} Our findings align with previous studies analyzing b-value variations in the Himalayas. Chetia *et al.*,⁴⁹ for example, observed b-value varying from 0.4 to 3.3 on the Himalayan and forehead region from 1964 to 2020.

The low b-value zones of the Himalayan region, extending from west to east, demonstrate a significant increase in seismic hazard potential (Figure 4).

In the Far Western Himalayas (72°E – 76°E) (Figure 4A), significant stress accumulation ($b = 0.7 - 0.9$) is noted in Himachal Pradesh, historically associated with the 1905 Kangra earthquake (Mw 7.8), where locked parts of the MHT maintain localized strain.⁶⁰ Proceeding eastward, the Western Himalayas (76°E – 80°E) (Figure 4B) display the sub-region's minimal b-values (0.6 – 0.7) in Uttarakhand (77°E – 79°E), which correlate with the Main Central Thrust and its rupture history, encompassing the 1991 Uttarkashi (Mw 6.8) and 1999 Chamoli (Mw 6.4) earthquakes.^{23,58,61} Further east, the Central-I Himalayas (80.5°E – 82.5°E) (Figure 4C) in mid-western Nepal exhibit significantly low b-values (0.6 – 0.65), indicating unruptured segments of the MHT that have preserved residual stress following the 2015 Gorkha earthquake (Mw 7.8).⁶² In proximity to this, the Central-II Himalayas (83°E – 88°E) (Figure 4D) exhibit a pronounced disparity: The western sector (83°E – 85°E) (Figure 4B) saw post-2015 stress release ($b = 0.9 - 1.05$), but the eastern sector (85°E – 88°E) retains low b-values (0.65 – 0.8), indicating persistent strain accumulation in central Nepal. The Eastern Himalayas (89°E – 95°E) (Figure 4D) are the most hazardous, with Bhutan's DCFZ gap (91°E – 93°E) exhibiting the lowest b-values (0.65 – 0.75) in the entire region.²⁴ This seismic gap, which has remained unruptured since the 1934

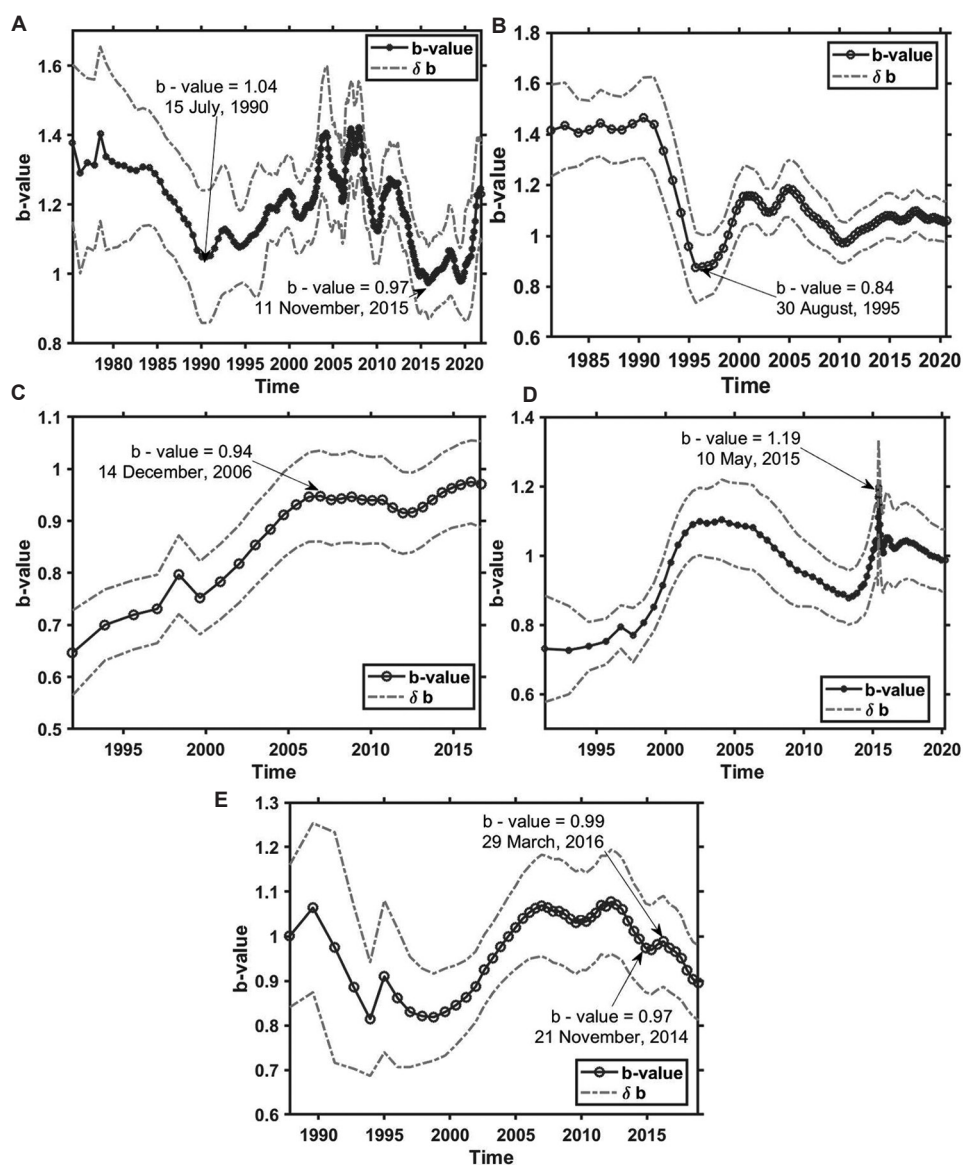


Figure 3. A time series analyzing b-value across Far Western Himalayan region (A), Western Himalayan Region (B), Central-I Himalayan Region (C), Central-II Himalayan Region (D), and Eastern Himalayan Region (E)

Bihar-Nepal earthquake, contains significant stress on the MHT, indicating an immediate threat of a mega-thrust event.⁶³ The west-to-east gradient from moderate strain to catastrophic potential highlights the Himalayas' dynamic

tectonic interactions, driven by the Indian and Eurasian plates' continuous convergence (~20 mm/year). Thus, monitoring and disaster resilience are crucial in high-risk areas, such as Bhutan and central Nepal.

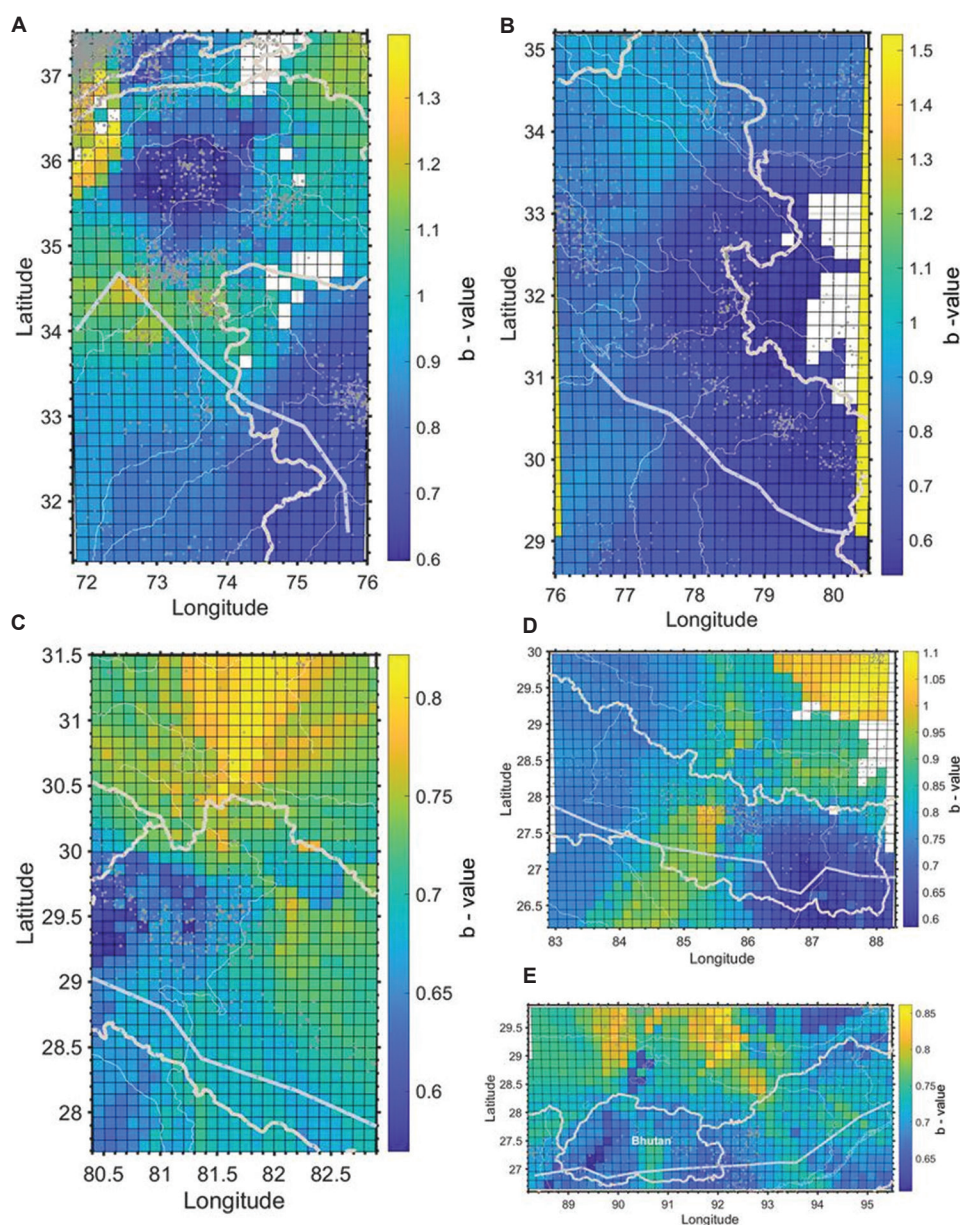


Figure 4. Spatial distribution of b-values across Far Western Himalayan region (A), Western Himalayan Region (B), Central-I Himalayan Region (C), Central-II Himalayan Region (D), and Eastern Himalayan Region (E)

4. Conclusion

In this study, earthquake data were obtained from the International Seismological Centre catalogue covering the Himalayan arc region between 71.6°E and 95.5°E for the period 1964 – 2023. The analysis was based on body-wave magnitude (mb), and to ensure accuracy, dependent events (foreshocks and aftershocks) were removed using the Reasenberg de-clustering algorithm implemented in MATLAB, allowing for the evaluation of only independent events (mainshocks).

The results of the investigation demonstrate clear spatial and temporal changes in b-values across distinct Himalayan sub-regions. Among the five zones investigated, the Far Western Himalayas demonstrated the greatest b-value (0.93 ± 0.02), which predicts a lower amount of tectonic stress accumulation and a dominance of small-magnitude earthquakes. In contrast, the Eastern Himalayas and Central-I region had the lowest b-values (0.68 ± 0.02 and 0.69 ± 0.03 , respectively), indicating a higher accumulation of stress and a greater likelihood of big, devastating seismic occurrences.

Temporal analysis showed dynamic changes in b-values over time. For instance, the b-value in the Far Western Himalayas decreased from 1.04 in 1990 to 0.97 in 2015, reflecting increasing tectonic strain before the 2015 Gorkha earthquake (Mw 7.8). Similarly, the Western Himalayas recorded a b-value of 0.84 in 1995, which was associated with subsequent major earthquakes, including the 1991 Uttarkashi (Mw 6.8) and 1999 Chamoli (Mw 6.4) events. The Central-II region showed a sharp increase in b-value to 1.19 during 2015, attributed to stress release from aftershock activity. Notably, the Dhubri-Chungthang seismic gap in Bhutan, with a persistent b-value of 0.65 – 0.75, remains unruptured since the 1934 Bihar-Nepal earthquake (Mw 8.4), indicating a silent but critical accumulation of strain, potentially making it a future earthquake hotspot.

The interpretation of these results is significant. Low b-values point to regions with high stress accumulation and fewer small earthquakes, which are more prone to host large seismic events. Conversely, high b-values indicate frequent small earthquakes and lower potential for major seismic rupture. The temporal decrease in b-values in certain regions can serve as a potential indicator of impending earthquakes, whereas post-event increases often reflect stress release through aftershocks.

This work sheds light on the spatial and temporal patterns of seismicity over the Himalayan region. It helps to improve seismic hazard assessment and disaster risk mitigation strategies by identifying high-stress and earthquake-prone areas. The findings emphasize the significance of ongoing monitoring, particularly in low b-value zones, such as the DCFZ gap, and call for increased earthquake preparedness and mitigation activities in these susceptible locations.

Acknowledgments

We would like to acknowledge Birendra Multiple Campus, Tribhuvan University, Bharatpur, Chitwan, Nepal, for providing a conducive research environment.

Funding

None.

Conflict of interest

The authors declare that the research was conducted in the absence of any commercial or financial relationships that could be construed as a potential conflict of interest.

Author contributions

Conceptualization: Ram Krishna Tiwari

Formal analysis: Ram Krishna Tiwari

Investigation: Ram Krishna Tiwari

Methodology: Ram Krishna Tiwari

Supervision: Harihar Paudyal

Visualization: Anil Subedi, Dilip Parajuli, Santosh Dharel,

Anil Neupane, Hari Subedi, Bishow Raj Timsina

Writing – original draft: Anil Subedi, Dilip Parajuli, Santosh Dharel, Anil Neupane, Hari Subedi, Bishow Raj Timsina

Writing – review and editing: Ram Krishna Tiwari, Harihar Paudyal

Availability of data

Data are freely available from the websites of the International Seismological Center.

References

- DiPietro JA, Pogue KR. Tectonostratigraphic subdivisions of the Himalaya: A view from the west. *Tectonics*. 2004;23(5):1-20.
doi: 10.1029/2003TC001554
- Molnar P, Tapponnier P. Cenozoic tectonics of Asia: Effects of a continental collision: Features of recent continental tectonics in Asia can be interpreted as results of the India-Eurasia collision. *Science*. 1975;189(4201):419-426.
doi: 10.1126/science.189.4201.419
- Martin CR, Jagoutz O, Upadhyay R, *et al.* Paleocene latitude of the Kohistan-Ladakh arc indicates multistage India-Eurasia collision. *Proc Natl Acad Sci U S A*. 2020;117(47):29487-29494.
doi: 10.1073/pnas.2009039117
- Meigs AJ, Burbank DW, Beck RA. Middle-late miocene (>10 Ma) formation of the main boundary thrust in the western Himalaya. *Geology*. 1995;23(5):423-426.
doi: 10.1130/0091-7613(1995)023<0423:MLMMFO>2.3.CO;2
- Valdiya KS. The two intracrustal boundary thrusts of the Himalaya. *Tectonophysics*. 1980;66(4):323-348.
doi: 10.1016/0040-1951(80)90248-6
- Bilham R, Larson K, Freymueller J, *et al.* GPS measurements of present-day convergence across the Nepal Himalaya. *Nature*. 1997;386(6620):61-64.
doi: 10.1038/386061a0
- Bilham R, Ambraseys N. Apparent Himalayan slip deficit from the summation of seismic moments for Himalayan earthquakes, 1500-2000. *Curr Sci*. 2005;88(10):1658-1663.
- Bilham R. Himalayan earthquakes: A review of historical seismicity and early 21st century slip potential. *Geol Soc Spec Publ*. 2019;483(1):423-482.
doi: 10.1144/SP483.16

9. Houston H. An introduction to seismology, earthquakes, and earth structure. *Phys Today*. 2003;56(10):66-67.
doi: 10.1063/1.1629009
10. Boulanouar A, Tiwari RK, Ahmed Z, Paudyal H. Fractal characteristics of earthquake occurrence in Al Hoceima city and its adjoining region, Morocco. *Geosyst Geoenviron*. 2025;4(3):100402.
doi: 10.1016/j.geogeo.2025.100402
11. Bilham R. Earthquakes in India and the Himalaya: Tectonics, geodesy and history. *Ann Geophys*. 2021;47(2-3):839-858.
doi: 10.4401/ag-3338
12. Kumar S, Wesnousky SG, Rockwell TK, Briggs RW, Thakur VC, Jayangondaperumal R. Paleoseismic evidences of grate surface rupture earthquakes along the Indian Himalaya. *J Geophys Res Solid Earth*. 2006;111(3):B03304.
doi: 10.1029/2004JB003309
13. Sapkota SN, Bollinger L, Klinger Y, Tapponnier P, Gaudemer Y, Tiwari D. Primary surface ruptures of the great Himalayan earthquakes in 1934 and 1255. *Nat Geosci*. 2013;6(1):71-76.
doi: 10.1038/ngeo1669
14. Bollinger L, Sapkota SN, Tapponnier P, *et al*. Estimating the return times of great Himalayan earthquakes in eastern Nepal: Evidence from the Patu and Bardibas strands of the Main Frontal Thrust. *J Geophys Res Solid Earth*. 2014;119(9):7123-7163.
doi: 10.1002/2014JB010970
15. Scordilis EM. Empirical global relations converting MS and mb to moment magnitude. *J Seismol*. 2006;10(2):225-236.
doi: 10.1007/s10950-006-9012-4
16. Tiwari RK, Paudyal H. Gorkha earthquake (MW7.8) and aftershock sequence: A fractal approach. *Earthq Sci*. 2022;35(3):193-204.
doi: 10.1016/j.eqs.2022.06.001
17. Reddy DV, Nagabhushanam P, Kumar D, *et al*. The great 1950 Assam Earthquake revisited: Field evidences of liquefaction and search for paleoseismic events. *Tectonophysics*. 2009;474(3-4):463-472.
doi: 10.1016/j.tecto.2009.04.024
18. Singh I, Pandey A, Mishra RL, *et al*. Evidence of the 1950 great assam earthquake surface break along the mishmi thrust at namche barwa himalayan syntaxis. *Geophys Res Lett*. 2021;48(11):1-9.
doi: 10.1029/2020GL090893
19. Kaneda H, Nakata T, Tsutsumi H, *et al*. Surface rupture of the 2005 Kashmir, Pakistan, earthquake and its active tectonic implications. *Bull Seismol Soc Am*. 2008;98(2):521-557.
doi: 10.1785/0120070073
20. Avouac JP, Ayoub F, Leprince S, Konca O, Helmberger DV. The 2005, Mw 7.6 Kashmir earthquake: Sub-pixel correlation of ASTER images and seismic waveforms analysis. *Earth Planet Sci Lett*. 2006;249(3-4):514-528.
doi: 10.1016/j.epsl.2006.06.025
21. Avouac JP, Meng L, Wei S, Wang T, Ampuero JP. Lower edge of locked Main Himalayan Thrust unzipped by the 2015 Gorkha earthquake. *Nat Geosci*. 2015;8(9):708-711.
doi: 10.1038/ngeo2518
22. Elliott JR, Jolivet R, Gonzalez PJ, *et al*. Himalayan megathrust geometry and relation to topography revealed by the Gorkha earthquake. *Nat Geosci*. 2016;9(2):174-180.
doi: 10.1038/ngeo2623
23. Tiwari RK, Chaudhary S, Paudyal H, Shanker D. Identifying seismicity pattern before major earthquakes in the Western Nepal and adjoining region (28.5°N to 31.0°N - 78°E to 82.96°E). *Environ Earth Sci*. 2024;83(15):1-11.
doi: 10.1007/s12665-024-11764-2
24. Diehl T, Singer J, Hetényi G, *et al*. Seismotectonics of Bhutan: Evidence for segmentation of the Eastern Himalayas and link to foreland deformation. *Earth Planet Sci Lett*. 2017;471:54-64.
doi: 10.1016/j.epsl.2017.04.038
25. Sciences P, Sciences A, Hall P, Nazionale I, Murata V. *Seismic Fault Rheology and Earthquake Dynamics. Tecton Faults*. Massachusetts: Massachusetts Institute of Technology; 2018.
doi: 10.7551/mitpress/6703.003.0007
26. Pudi R, Tapas RM, Vinod KK. Regional variation of stress level in the Himalayas after the 25 April 2015 Gorkha earthquake (Nepal) estimated using b-values. *J Geophys Eng*. 2018;15(3):921-927.
doi: 10.1088/1742-2140/aaa26c
27. Bhatia SC, Kumar MR, Gupta HK. A probabilistic seismic hazard map of India and adjoining regions. *Ann di Geofis*. 1999;42(6):1153-1164.
doi: 10.4401/ag-3777
28. Das S, Gupta ID, Gupta VK. A probabilistic seismic hazard analysis of Northeast India. *Earthq Spectra*. 2006;22(1):1-27.
doi: 10.1193/1.2163914
29. Gutenberg B, Richter CFF. Frequency of earthquakes in California. *Bull Seismol Soc Am*. 1944;34:185-188.
doi: 10.1038/156371a0
30. Okal EA, Romanowicz BA. On the variation of b-values with earthquake size. *Phys Earth Planet Inter*. 1994;87(1-2):55-76.
doi: 10.1016/0031-9201(94)90021-3
31. Scholz CH. On the stress dependence of the earthquake b value. *Geophys Res Lett*. 2015;42(5):1399-1402.
doi: 10.1002/2014GL062863

32. Wiemer S, Wyss M. Mapping spatial variability of the frequency-magnitude distribution of earthquakes. *Adv Geophys.* 2002;45(C):259-302.
doi: 10.1016/S0065-2687(02)80007-3
33. Nakaya S. Spatiotemporal variation in b value within the subducting slab prior to the 2003 Tokachi-oki earthquake (M 8.0), Japan. *J Geophys Res Solid Earth.* 2006;111(3):3311.
doi: 10.1029/2005JB003658
34. Sharma V, Bora DK, Biswas R. Spatio-temporal analysis of b-value prior to 28 April 2021 Assam Earthquake and implications thereof. *Ann Geophys.* 2022;65(5):SE534.
doi: 10.4401/ag-8802
35. Tiwari RK, Paudyal H. Variability of b-value before and after the Gorkha earthquake in the Central Himalaya and Vicinity. *BIBECHANA.* 2021;18(2):32-42.
doi: 10.3126/bibechana.v18i2.31207
36. Bondár I, Storchak D. Improved location procedures at the international seismological centre. *Geophys J Int.* 2011;186(3):1220-1244.
doi: 10.1111/j.1365-246X.2011.05107.x
37. Willemann RJ, Storchak DA. Data collection at the international seismological centre. *Seismol Res Lett.* 2001;72(4):440-453.
doi: 10.1785/gssrl.72.4.440
38. Di Giacomo D, Robert Engdahl E, Storchak DA. The ISC-GEM Earthquake Catalogue (1904-2014): Status after the extension project. *Earth Syst Sci Data.* 2018;10(4):1877-1899.
doi: 10.5194/essd-10-1877-2018
39. Reasenber P. Second-order moment of central California seismicity, 1969-1982. *J Geophys Res Solid Earth.* 1985;90(B7):5479-5495.
doi: 10.1029/jb090ib07p05479
40. Wiemer S, Wiemer. A software package to analyze seismicity: ZMAP. *Seismol Res Lett.* 2001;72(3):373-382.
doi: 10.1785/gssrl.72.3.373
41. Aki K. Maximum likelihood estimate of b in the Gutenberg-Richter formula and its confidence limits. *Bull Earthq Res Inst.* 1965;43(43):237-239.
42. Utsu T. Aftershocks and earthquake statistics (III)- analyses of the distribution of earthquakes in magnitude, time, and space with special consideration to clustering characteristics of earthquake occurrence (1). *J Fac Sci Hokkaido Univ Ser VII.* 1971;3:379-441.
43. Shi Y, Bolt BA. The standard error of the magnitude-frequency b value. *Bull Seismol Soc Am.* 1982;72(5):1677-1687.
doi: 10.1785/bssa0720051677
44. Tiwari RK, Paudyal H. Fractal characteristics of the seismic swarm succeeding the 2015 Gorkha Earthquake, Nepal. *Indian Geotech J.* 2023;53(4):789-804.
doi: 10.1007/s40098-022-00704-1
45. Aswini KK, Kamesh Raju KA, Dewangan P, Yattheesh V, Singha P, Ramakrushana Reddy T. Seismotectonic evaluation of off Nicobar Earthquake Swarms, Andaman Sea. *J Asian Earth Sci.* 2021;221:104948.
doi: 10.1016/j.jseaes.2021.104948
46. Oncel AO, Wilson T. Space-time correlations of seismotectonic parameters: Examples from Japan and from Turkey preceding the İzmit earthquake. *Bull Seismol Soc Am.* 2002;92(1):339-349.
doi: 10.1785/0120000844
47. Babu VG, Kumar N, Verma SK, Pal SK. An updated earthquake catalogue and seismic regimes in the northwest Himalaya: Seismic periodicity associated with strong earthquakes. *J Earth Syst Sci.* 2023;132(4):173.
doi: 10.1007/s12040-023-02180-4
48. Khan PK, Mohanty SP, Sinha S, Singh D. Occurrences of large-magnitude earthquakes in the Kachchh region, Gujarat, western India: Tectonic implications. *Tectonophysics.* 2016;679:102-116.
doi: 10.1016/j.tecto.2016.04.044
49. Chetia M, Gogoi PR, Lahiri SK. Temporal variation of seismic b-value in the Himalayas and foreland region and its implications on crustal stress variability. *Acta Geophys.* 2023;71(4):1675-1692.
doi: 10.1007/s11600-022-00999-x
50. Tiwari RK, Paudyal H. Analysis of the b, p values, and the fractal dimension of aftershocks sequences following two major earthquakes in central Himalaya. *Heliyon.* 2024;10(2):e24476.
doi: 10.1016/j.heliyon.2024.e24476
51. Molnar P, Lyon-Caen H. Fault plane solutions of earthquakes and active tectonics of the Tibetan Plateau and its margins. *Geophys J Int.* 1989;99(1):123-154.
doi: 10.1111/j.1365-246X.1989.tb02020.x
52. Tiwari RK, Paudyal H. Spatial mapping of b-value and fractal dimension prior to November 8, 2022 Doti Earthquake, Nepal. *PLoS One.* 2023;18:e0289673.
doi: 10.1371/journal.pone.0289673
53. Kumar S, Sharma N. The seismicity of central and north-east Himalayan region. *Contrib Geophys Geodes.* 2019;49(3):265-281.
doi: 10.2478/congeo-2019-0014
54. Pathak V, Pant C, Joshi S. Source Parameter and b-Value Estimation of Local Earthquakes in Kumaun Region, Central Himalaya, India. *Int J Adv Res.* 2016;4(9):15254-1266.

- doi: 10.21474/ijar01/1609
55. Yadav RBS, Bormann P, Rastogi BK, Das MC, Chopra S. A homogeneous and complete earthquake catalog for northeast India and the adjoining region. *Seismol Res Lett.* 2009;80(4):609-627.
doi: 10.1785/gssrl.80.4.609
 56. Rajendran K, Parameswaran RM, Rajendran CP. Revisiting the 1991 Uttarkashi and the 1999 Chamoli, India, earthquakes: Implications of rupture mechanisms in the central Himalaya. *J Asian Earth Sci.* 2018;162:107-120.
doi: 10.1016/j.jseaes.2018.04.012
 57. Tiwari A, Paul A, Singh R, Upadhyay R. Potential seismogenic asperities in the Garhwal-Kumaun region, NW Himalaya: Seismotectonic implications. *Nat Hazards.* 2021;107(1):73-95.
doi: 10.1007/s11069-021-04574-3
 58. Yadav RBS, Koravos GC, Tsapanos TM, Vougiouka GE. A probabilistic estimate of the most perceptible earthquake magnitudes in the NW Himalaya and Adjoining Regions. *Pure Appl Geophys.* 2015;172(2):197-212.
doi: 10.1007/s00024-014-0864-1
 59. Gunti S, Roy P, Narendran J, *et al.* Assessment of geodetic strain and stress variations in Nepal due to 25 April 2015 Gorkha earthquake: Insights from the GNSS data analysis and b-value. *Geod Geodyn.* 2022;13(3):288-300.
doi: 10.1016/j.geog.2022.01.003
 60. Hajra S, Hazarika D, Shukla V, Kundu A, Pant CC. Stress dissipation and seismic potential in the central seismic gap of the north-west Himalaya. *J Asian Earth Sci.* 2022;239:105432.
doi: 10.1016/j.jseaes.2022.105432
 61. Prasath RA, Paul A, Singh S. Earthquakes in the garhwal himalaya of the central seismic gap: A study of historical and present seismicity and their implications to the seismotectonics. *Pure Appl Geophys.* 2019;176(11):4661-4685.
doi: 10.1007/s00024-019-02239-8
 62. Sreejith KM, Sunil PS, Agrawal R, Saji AP, Rajawat AS, Ramesh DS. Audit of stored strain energy and extent of future earthquake rupture in central Himalaya. *Sci Rep.* 2018;8(1):1-9.
doi: 10.1038/s41598-018-35025-y
 63. Rajendran K, Parameswaran RM, Rajendran CP. Seismotectonic perspectives on the Himalayan arc and contiguous areas: Inferences from past and recent earthquakes. *Earth-Science Rev.* 2017;173:1-30.
doi: 10.1016/j.earscirev.2017.08.003